Clinical Trials: Targeted Therapy

Clinical Cancer Research

Sorafenib Population Pharmacokinetics and Skin Toxicities in Children and Adolescents with Refractory/Relapsed Leukemia or Solid Tumor Malignancies

Hiroto Inaba[1,2], John C. Panetta[3], Stanley B. Pounds[4], Lei Wang[4], Lie Li[3], Fariba Navid[5], Sara M. Federico[1,2], Eric D. Eisenmann[6], Aksana Vasilyeva[7], Yong-Dong Wang[8], Sheila Shurtleff[9], Ching-Hon Pui[1,2,9], Tanja A. Gruber[1,2,9], Raul C. Ribeiro[1,2], Jeffrey E. Rubnitz[1,2], and Sharyn D. Baker[6]

Abstract

Purpose: To determine the pharmacokinetics and skin toxicity profile of sorafenib in children with refractory/relapsed malignancies.

Patients and Methods: Sorafenib was administered concurrently or sequentially with clofarabine and cytarabine to patients with leukemia or with bevacizumab and cyclophosphamide to patients with solid tumor malignancies. The population pharmacokinetics (PPK) of sorafenib and its metabolites and skin toxicities were evaluated.

Results: In PPK analysis, older age, bevacizumab and cyclophosphamide regimen, and higher creatinine were associated with decreased sorafenib apparent clearance (CL/f; $P<0.0001$ for all), and concurrent clofarabine and cytarabine administration was associated with decreased sorafenib N-oxide CL/f ($P = 7e{-}4$). Higher bilirubin was associated with decreased sorafenib N-oxide and glucuronide CL/f ($P = 1e{-}4$). Concurrent use of organic anion-transporting polypeptide 1B1 inhibitors was associated with increased sorafenib and decreased sorafenib glucuronide CL/f ($P<0.003$). In exposure–toxicity analysis, a shorter time to development of grade 2–3 hand–foot skin reaction (HFSR) was associated with concurrent ($P = 0.0015$) but not with sequential ($P = 0.59$) clofarabine and cytarabine administration, compared with bevacizumab and cyclophosphamide, and with higher steady-state concentrations of sorafenib ($P = 0.0004$) and sorafenib N-oxide ($P = 0.0275$). In the Bayes information criterion model selection, concurrent clofarabine and cytarabine administration, higher sorafenib steady-state concentrations, larger body surface area, and previous occurrence of rash appeared in the four best two-predictor models of HFSR. Pharmacokinetic simulations showed that once-daily and every-other-day sorafenib schedules would minimize exposure to sorafenib steady-state concentrations associated with HFSR.

Conclusions: Sorafenib skin toxicities can be affected by concurrent medications and sorafenib steady-state concentrations. The described PPK model can be used to refine exposure–response relations for alternative dosing strategies to minimize skin toxicity.

[1]Department of Oncology, St. Jude Children's Research Hospital, Memphis, Tennessee. [2]Department of Pediatrics, University of Tennessee Health Science Center, Memphis, Tennessee. [3]Department of Pharmaceutical Sciences, St. Jude Children's Research Hospital, Memphis, Tennessee. [4]Department of Biostatistics, St. Jude Children's Research Hospital, Memphis, Tennessee. [5]Children's Hospital of Los Angeles, University of Southern California, Keck School of Medicine, Los Angeles, California. [6]Division of Pharmaceutics and Pharmacology, College of Pharmacy and Comprehensive Cancer Center, The Ohio State University, Columbus, Ohio. [7]Cancer Center Administration, St. Jude Children's Research Hospital, Memphis, Tennessee. [8]Department of Computational Biology, St. Jude Children's Research Hospital, Memphis, Tennessee. [9]Department of Pathology, St. Jude Children's Research Hospital, Memphis, Tennessee.

Note: Supplementary data for this article are available at Clinical Cancer Research Online (http://clincancerres.aacrjournals.org/).

H. Inaba and J.C. Panetta contributed equally to this article.

Corresponding Author: Hiroto Inaba, St. Jude Children's Research Hospital, 262 Danny Thomas Place, Memphis, TN 38105. Phone: 901-595-3300; Fax: 901-521-9005; E-mail: hiroto.inaba@stjude.org

Clin Cancer Res 2019;25:7320–30

doi: 10.1158/1078-0432.CCR-19-0470

Introduction

Acute myeloid leukemia (AML) accounts for approximately 20% of the acute leukemias in children and adolescents (1, 2). Although the overall survival rate in patients with AML is improving, 30% to 40% of patients experience recurrence, which is associated with poor prognosis and survival rates of less than 30%. Similarly, whereas the overall survival of children with solid tumor malignancies is approximately 75%, that for children with recurrent or metastatic solid tumors is also below 30% (3). For better salvage of such patients and to improve first-line therapy, newer agents with different mechanisms of action are needed.

Sorafenib is an orally available multikinase inhibitor that blocks pathways with possible roles in the development and progression of AML and solid tumor malignancies, involving C-RAF, B-RAF, c-KIT, FMS-like tyrosine kinase 3 (FLT3), platelet-derived growth factor receptors α and β, vascular endothelial growth factor receptors 1–3, or multiple intracellular kinases (4, 5). Sorafenib is metabolized, in part, to the active metabolite sorafenib N-oxide by cytochrome P450 3A4 (CYP3A4) and to sorafenib glucuronide by uridine diphosphate-glucuronosyltransferase family 1 member

Translational Relevance

As approximately 30% of pediatric cancer recurs, new therapeutic agents with different mechanisms of action are needed. This study examined the pharmacokinetics and skin toxicity profile in pediatric patients of the multikinase inhibitor sorafenib in combination with clofarabine and cytarabine (for relapsed/refractory leukemia) or bevacizumab and cyclophosphamide (for solid tumor malignancies). Concurrent administration of sorafenib with clofarabine and cytarabine was associated with severe skin toxicities, whereas sequential administration of sorafenib with clofarabine and cytarabine or a lower dose of sorafenib in combination with bevacizumab and cyclophosphamide was well tolerated. A population pharmacokinetic model identified covariates affecting the apparent clearance and steady-state exposure of sorafenib and its metabolites. Patients experiencing grade $\geq$2 hand–foot skin reaction, as compared with those with grade 0–1, had higher steady-state trough concentrations of sorafenib and sorafenib N-oxide. The described population pharmacokinetic model can be used to refine exposure–response relations and develop alternative dosing strategies for sorafenib to minimize skin toxicity.

A9 (UGT1A9; ref. 6). Clinical studies have demonstrated the efficacy of sorafenib as a single agent or in combination with cytotoxic chemotherapy in treating pediatric and adult AML (7–11). Sorafenib is approved for treating adults with hepatocellular carcinoma, renal cell carcinoma, and differentiated thyroid cancer (12–15). We have previously reported that sorafenib administered concurrently with clofarabine and cytarabine showed activity in children and adolescents with relapsed or refractory AML, especially in those with FLT3-internal tandem duplication (FLT3-ITD; ref. 9). In addition, antitumor activity of sorafenib alone or in combination with bevacizumab and cyclophosphamide was seen in recurrent/refractory pediatric solid tumors (16, 17). However, hand–foot skin reaction (HFSR) and/or skin rash were frequent side effects of sorafenib treatment and were exacerbated by the administration of concomitant agents (9, 17–22). These dermatologic adverse effects, especially HFSR, are associated with poor quality of life, and their pathogenesis and strategies for prevention and optimum supportive care are unclear (23).

To develop better management for children treated with sorafenib, we evaluated the pharmacokinetics and skin toxicity profile of the drug in pediatric patients with relapsed/refractory leukemia or solid tumor malignancies.

Patients and Methods

Patients

Patients aged $\leq$31 years with relapsed or refractory leukemia and those with relapsed or refractory solid tumors aged $\leq$21 years at the time of original diagnosis, irrespective of the number of prior salvage regimens, were eligible for the protocols RELHEM (NCT00908167) and ANGIO1 (NCT00665990), respectively, as described previously (9, 17). The protocols were approved by the institutional review board of St. Jude Children's Research Hospital (Memphis, TN) and the studies were conducted in accordance with Declaration of Helsinki. Written informed consent was obtained from all patients or from their legal guardians with assent from the patients as appropriate.

Treatment plan

The first 12 patients enrolled on RELHEM received deescalating doses of sorafenib (on days 1–28) and clofarabine and cytarabine (on days 8–12) together (the concurrent regimen) at the dose levels shown in Supplementary Table S1 and described previously (9). In subsequent cohorts of patients, sorafenib was administered sequentially with clofarabine and cytarabine (the sequential regimen) with interpatient dose escalation of clofarabine or deescalation of clofarabine or sorafenib (Supplementary Table S1). In the sequential regimen, sorafenib was administered on days 1 to 7 and days 15 to 28 and clofarabine and cytarabine were administered once daily on days 8 to 12. Once the MTD was established, enrollment was expanded to 12 additional patients to enable further assessment of the toxicity, pharmacokinetics, and efficacy.

The first cohort of patients for ANGIO1 received escalating doses of sorafenib (on days 1–21) with fixed doses of bevacizumab (on day 1) and cyclophosphamide (on days 1–21; Supplementary Table S1; ref. 17). Once an MTD of sorafenib was established, the bevacizumab dose was escalated. After the MTD had been established, enrollment was expanded by up to 25 additional patients with solid tumors or hematologic malignancies.

Toxicity criteria

The Common Terminology Criteria for Adverse Events (CTCAE) Version 3.0 was used for toxicity evaluations. Dose-limiting toxicities (DLT) were evaluated in the first course and included any grade 3 or higher nonhematologic toxicities related to therapy except for the following: grade 3 elevations of amylase, lipase, or total bilirubin or grade 3 or 4 elevations of alanine aminotransferase (ALT) and aspartate aminotransferase (AST) that resolved within 7 days of holding sorafenib; grade 3 hypokalemia, hypocalcemia, hypophosphatemia, or hypomagnesemia that was correctable with oral supplements; grade 3 hypertension that was well controlled with oral medication; or grade 3 or 4 infection or fever, as described previously (9, 17). For HFSR, grades and symptoms were based on the 2008 consensus panel recommendations (24).

Sorafenib pharmacokinetic studies

For the concurrent regimen of RELHEM, blood samples were collected before and at 2, 4.5, and 7.5 hours after sorafenib administration on days 7 and 12 of course 1. For the sequential regimen, blood samples were obtained before and at 0.5, 1, 2, 4, 6, 8, and 24 hours after sorafenib administration on day 1; the evening dose of sorafenib was held on day 1 to permit pharmacokinetic assessments. Serial blood samples were also obtained on day 7, and a pretreatment trough concentration was obtained on day 15 $\pm$ 2 days for the sequential regimen.

In the ANGIO1 protocol, samples were collected before the first dose of sorafenib on day 1 and at 0.5, 2, 4.5, 6, 7.5, 24, and 48 hours after sorafenib administration. After the first dose, sorafenib was withheld until the morning of day 3 (after the blood sample at 48 hours was obtained). Blood samples were also obtained during course 1 before sorafenib treatment on days 7, 13, and 21.

The concentrations of sorafenib, sorafenib N-oxide, and sorafenib glucuronide were measured in plasma (heparinized) by using a validated HPLC-based method with tandem mass spectrometric detection (6).

Pharmacokinetic data analysis

The PPK and individual *post hoc* estimates of sorafenib, sorafenib N-oxide, and sorafenib glucuronide were determined by nonlinear mixed-effects modeling with NONMEM 7.3 (ICON Development Solutions), using the iterative two-stage, stochastic approximation expectation-maximization, and importance sampling methods, sequentially. A linear three-compartment model (one compartment for each component) with zero-order absorption, an absorption lag time, and first-order elimination was used to model the data. A diagram of the model along with the parameters estimated is shown in Supplementary Fig. S1. In addition, the individual *post hoc* parameter values were used to estimate the AUC, the maximum concentration (C_{max}), and the steady-state (SS) trough concentration on day 7 of therapy (i.e., the concentration immediately before the first dose on day 7) for sorafenib, sorafenib N-oxide, and sorafenib glucuronide. Each individual's pharmacokinetic study was subdivided into two occasions. Occasion 1 was the first serially sampled pharmacokinetic study in each individual. This was day 1 (after the first dose of sorafenib) in all individuals except those on RELHEM with concurrent treatment, for whom this occurred on day 7 with 4 serial samples. Occasion 2 included samples after the serially sampled study to the end of the course. This typically occurred on day 7 (for those who had a pharmacokinetic study on day 1), along with trough samples on days 14 and 21. The interindividual variability (IIV) and interoccasion variability (IOV) of the parameters was assumed to be log-normally distributed. A proportional residual error model was used with assumed normal distribution of the residuals.

The covariates age, body surface area (BSA), serum chemistries (ALT, AST, albumin, alkaline phosphatase, bilirubin, and creatinine), estimated glomerular filtration rate via the St. Jude equation (25), concomitant medications that were inhibitors of organic anion-transporting polypeptide (OATP) 1B1 (micafungin, vancomycin, and posaconazole; refs. 26–28), study day (day 1 vs. day 7), study protocol (RELHEM vs. ANGIO1), and concurrent use of clofarabine and cytarabine in RELHEM versus other regimens (sequential use of clofarabine and cytarabine in RELHEM and ANGIO1) were evaluated to determine their significance in explaining pharmacokinetic variability. These covariates were considered significant in a univariate analysis if their addition to the model reduced the objective function value (OFV) by at least 3.84 units ($P < 0.05$, based on the χ^2 test for the difference in the -2 log-likelihood between two hierarchical models that differ by 1 degree of freedom) and if the covariate term was significantly different from zero ($P < 0.05$ by a t test).

Exposure–toxicity association analysis

Cox proportional hazard models were used to evaluate the association of the time from starting sorafenib treatment until the first occurrence of grade 2 or higher HFSR with the following clinical and pharmacologic variables: treatment regimen (concurrent regimen in RELHEM or sequential regimen in RELHEM vs. ANGIO1), age, BSA, incidence of grade 2 or higher rash (as a time-dependent predictor indicating whether rash has previously occurred), and the SS trough levels of sorafenib, sorafenib N-oxide, and sorafenib glucuronide. Each of these variables was first evaluated as the sole predictor in a Cox model. Then, all possible models with two of these variables were considered and evaluated with the Bayes information criterion (BIC). BIC values were transformed into evidence weights that represented the probability of being the best model among the considered set of models (29). Because the sorafenib glucuronide SS trough concentration was available only for a subset of individuals (55 of 74), it was not considered in the BIC model selection analysis. Individuals were considered censored at the end of the course or when sorafenib therapy was stopped. In addition, Fine–Gray models were used to evaluate factors that were associated with the development of grade 2 or higher rash, treating development of grade 2 or higher HFSR before rash as a competing event. Rash was modeled as a time-dependent covariate predicting HFSR, and HFSR was modeled as a competing event for rash because sorafenib was primarily discontinued for HFSR.

Results

Patient characteristics

The clinical features of the 37 patients enrolled on RELHEM (12 patients on the concurrent regimen and 25 on the sequential regimen) and the 45 patients enrolled on ANGIO1 (19 patients in the dose-escalation phase and 26 in the expansion phase) are summarized in Supplementary Table S2.

Skin toxicities

As reported previously, among the 12 patients treated with the concurrent regimen of RELHEM (9), 2 of 4 patients in stratum 1 and 1 of 2 patients in stratum 2 had grade 3 HFSR and/or rash as DLTs with 200 mg/m^2 sorafenib (Table 1). All DLTs were due to skin toxicities. No DLTs were observed in stratum 1 with 150 mg/m^2 sorafenib (6 patients), but grade 2 HFSR (in 3 patients) and skin rash (in 3 patients) were still frequent at this dose level. Overall, HFSR and skin rash of grade 2 or higher were each observed in 8 (67%) of the 12 patients, respectively. In the 21 evaluable patients treated with the sequential regimen of RELHEM, HFSR and skin rash of grade 2 were seen in 4 patients (19%) and 6 patients (29%), respectively (Table 1). No DLTs, including grade 3 skin toxicities, were observed at any dose level, with dose level 3 (sorafenib, 200 mg/m^2 twice daily; clofarabine, 40 mg/m^2; and cytarabine, 1,000 mg/m^2), which was determined to be the MTD.

During the phase I portion of ANGIO1, 2 of 4 DLTs were HFSR (Table 1). Among 4 patients treated at the dose level 2, two patients had DLTs; one patient had grade 3 HFSR and the other experienced grade 3 elevated lipase (17). Therefore, the MTD for sorafenib was determined to be 90 mg/m^2/dose twice daily. At dose level 3 (in the bevacizumab escalation), one of 6 patients developed grade 3 thrombus, and at dose level 4, one of six patients developed grade 3 HFSR and anorexia. Although the MTD was not reached, the recommended phase II dose was defined as sorafenib 90 mg/m^2/dose twice daily, bevacizumab 15 mg/kg, and cyclophosphamide 50 mg/m^2/dose. Among the 19 patients in the phase I portion, 4 (21%) developed grade 2 ($n = 2$) or grade 3 ($n = 2$) HFSR, and three (16%) developed grade 2 rash. Among 26 patients treated in the expansion arm, 6 (23%) developed HFSR of grade 2 ($n = 4$) or grade 3 ($n = 2$). No grade 2 or higher skin rash was observed in the expansion arm.

Table 1. Skin toxicities in RELHEM (concurrent and sequential) and ANGIO 1 protocols

	Strata, dose level																			
	Stratum 1								Stratum 2											
	Dose level 1: sorafenib 200 mg/m^2 (*n* = 4)				Dose level 2: sorafenib 150 mg/m^2 (*n* = 6)				Dose level 1: sorafenib 200 mg/m^2 (*n* = 2)				All patients (*n* = 12)							
RELHEM (concurrent)																				
Grades	1	2	3	4	1	2	3	4	1	2	3	4	1	2	3	4				
HFSR		2	**2**			3					**1**			5	3					
Rash		2	**2**		2	3			1				2	6	2					
	Strata, dose level																			
	Dose-escalation strata												Expansion strata							
	Dose level 1: clofarabine 20 mg/m^2 (*n* = 3)				Dose level 2: clofarabine 30 mg/m^2 (*n* = 3)				Dose level 3: clofarabine 40 mg/m^2 (*n* = 6)				Clofarabine 40 mg/m^2 (*n* = 9)				All patients (*n* = 21)			
RELHEM (sequential)																				
Grades	1	2	3	4	1	2	3	4	1	2	3	4	1	2	3	4	1	2	3	4
HFSR						1			1	1				2			1	4		
Rash	2	1			1	1			2	2			1	2			6	6		
	Strata, dose level																			
	Dose-escalation strata												Expansion strata							
	Dose level 1: sorafenib 90 mg/m^2 (*n* = 3)				Dose level 2: sorafenib 110 mg/m^2 (*n* = 4)				Dose level 3: bevacizumab 10 mg/kg (*n* = 6)				Dose level 4: bevacizumab 15 mg/kg (*n* = 6)				Sorafenib 90 mg/m^2, bevacizumab 15 mg/kg (*n* = 26)				All patients (*n* = 45)			
ANGIO1																				
Grades	1	2	3	4	1	2	3	4	1	2	3	4	1	2	3	4	1	2	3	4
HFSR	1	1			2		**1**		1				1	1	**1**		6	4	2		11	6	4	
Rash	1				1	1			3				1	2			9				15	3		

NOTE: Bold letters show dose-limiting toxicities.

Sorafenib population pharmacokinetics

A total of 74 patients enrolled on either RELHEM (35 patients, 11 treated with the concurrent regimen and 24 with the sequential regimen) or ANGIO1 (39 patients) had evaluable pharmacokinetic studies in course 1. The PPK parameters for plasma concentrations of sorafenib (total number of plasma concentrations: $n = 721$), sorafenib N-oxide ($n = 662$), and sorafenib glucuronide ($n = 474$) for the base model (with only BSA-normalized parameters) are listed in Table 2, and their concentration-versus-time plots, along with the population-estimated curve for each individual study (the concurrent and sequential arms of RELHEM and ANGIO1) are shown in Fig. 1. In RELHEM, sorafenib day 12 exposures were maintained relative to the day 7 exposure with the concurrent regimen. With the sequential regimen, the sorafenib model-predicted day 12 exposures (after 5 days of stopping sorafenib for clofarabine and cytarabine administration), as well as the observed day 15 exposures, were up to three orders of magnitude lower than the corresponding exposures with the concurrent regimen. The sorafenib exposure in ANGIO1 was lower than that in RELHEM.

We evaluated each of the covariates and compared them to the base model. Among the covariates, age, study protocol (RELHEM vs. ANGIO1), concurrent administration with clofarabine and cytarabine (vs. others), bilirubin, creatinine, and OATP1B1 inhibitors, each significantly improved the model fit relative to the base model (Supplementary Table S3). OATP1B1 inhibitors were only given to RELHEM patients as infection prophylaxis (Supplementary Table S4). Sorafenib population apparent clearance decreased with increasing age from 3.8 L/hour/m^2 in a patient aged 1 year to 1.8 L/hour/m^2 in a patient aged 15 years ($P = 1e{-}5$), and the sorafenib population apparent clearance was 37% lower in ANGIO1 than in RELHEM ($P = 9e{-}5$; Fig. 2A). In addition, a sorafenib population apparent clearance of 3.1 L/hour/m^2 with a creatinine level of 0.2 mg/dL decreased to 1.5 L/hour/m^2 with a creatinine level of 0.8 mg/dL ($P = 7e{-}6$; Fig. 2B). Sorafenib N-oxide population apparent clearance was 65% lower in patients who received concurrent administration in RELHEM than in other patients ($P = 7e{-}4$; Fig. 2C). Sorafenib N-oxide and glucuronide population apparent clearance were also lower in patients with higher bilirubin, declining from 25.7 and 0.098 L/hour/m^2 when the bilirubin level was 0.2 mg/dL to 10.4 and 0.064 L/hour/m^2 when the bilirubin level was 1.0 mg/dL, respectively ($P = 1e{-}4$; Fig. 2D and E). Sorafenib population apparent clearance was 50% higher and the sorafenib glucuronide population apparent clearance was 22% lower in individuals who received OATP1B1 inhibitors ($P = 3e{-}3$; Fig. 2F and G). The covariates, age, study protocol, creatinine, and OATP1B1 inhibitors accounted for 22%, 43%, 59%, and 13%, respectively, of the IIV in sorafenib apparent clearance; concurrent administration with clofarabine and cytarabine and bilirubin accounted for 49% and 12%, respectively, of the IIV in sorafenib N-oxide apparent clearance; and bilirubin and OATP1B1 inhibitors accounted for 24% and 13%, respectively, of the IIV in sorafenib glucuronide apparent clearance.

We next considered combinations of covariates. Relative to the base model, the model that included age, study protocol (RELHEM vs. ANGIO1), and concurrent administration with clofarabine and cytarabine (vs. others) accounted for 67% of the IIV in sorafenib apparent clearance and 49% of the IIV in

Table 2. PPK parameters obtained from the base (body surface area normalized) and final covariate models

Parameters	Base estimate	RSE (CV %)	Final model estimate	RSE (CV %)
T_{lag} (h)	0.54	11.3	0.50	12.4
R_0 (μg/h/m^2)	44751.7	20.8	42473.9	23.5
V_1/f (L/m^2)	89.6	6.7	87.8	19.3
$Cl_{sorafenib}$/f (L/h/m^2)	2.14	9.3	2.46	14.3
β: Age—$Cl_{sorafenib}$	—	—	−0.23	52.8
β: Study—$Cl_{sorafenib}$	—	—	0.72	24.9
K_{13} (h^{-1})	0.00012	59.9	0.00017	70.1
V_2/fn (L/m^2)	14.7	28.6	17.0	35.4
$Cl_{N\text{-}oxide}$/fn (L/h/m^2)	18.3	15.0	18.6	19.3
β: CON—$Cl_{N\text{-}oxide}$	—	—	0.43	49.9
β: Bili—$Cl_{N\text{-}oxide}$	—	—	−0.35	73.1
V_3/fg (L/m^2)	0.047	60.5	0.073	71.0
$Cl_{glucuronide}$/fg (L/h/m^2)	0.049	61.3	0.066	66.6
β: Bili—$Cl_{glucuronide}$	—	—	−0.28	88.6
σ prop	0.098, 0.13, 0.043	9.5, 12.3, 19.3	0.10, 0.13, 0.044	12.6, 17.3, 42.5
−2 Log-likelihood	21352.7		21293.1	

	Variance		RSE (%)		Variance		RSE (%)	
	IIV	IOV	IIV	IOV	IIV	IOV	IIV	IOV
T_{lag}	0.36	—	34.3	—	0.34	—	42.7	—
R_0	1.2	—	24.1	—	1.1	—	29.1	—
V_1/f	0.087	0.16	46.9	50.7	0.072	0.17	87.6	90.7
$Cl_{sorafenib}$/f	0.15	0.18	45.2	24.6	0.059	0.048	83.5	30.8
K_{13}	0.21	0.18	59.0	99.3	0.13	0.39	70.5	223.0
V_2/fn	0.75	—	45.9	—	0.94	—	61.5	—
$Cl_{N\text{-}oxide}$/fn	0.39	0.59	49.7	28.0	0.22	0.23	82.4	42.4
V_3/fg	—	—	—	—	—	—	—	—
$Cl_{glucuronide}$/fg	0.28	—	44.9	—	0.23	—	83.1	—

NOTE: Covariate model: $\theta^{*}\exp(\beta^{*}\text{covariate})$ for continuous covariates and $\theta^{*}\beta^{\text{covariate}}$ for categorical covariates. The categorical variables are defined as follows: CON = [0—sequential dosing in RELHEM and ANGIO1 or 1—concurrent dosing in RELHEM] and Study = [0–RELHEM or 1–ANGIO1].

Abbreviations: $Cl_{glucuronide}$/fg (L/h/m^2), the sorafenib glucuronide apparent clearance where fg is the unidentifiable formation fraction; $Cl_{N\text{-}oxide}$/fn (L/h/m^2), the sorafenib N-oxide apparent clearance where fn is the unidentifiable formation fraction; $Cl_{sorafenib}$/f (L/h/m^2), the sorafenib apparent clearance where f is the unidentifiable bioavailability; K_{13} (h^{-1}), the sorafenib to sorafenib N-oxide rate constant; CV, coefficient of variation; σ prop, proportional residual error for sorafenib, sorafenib N-oxide, and sorafenib glucuronide, respectively; R_0 (μg/h/m^2), the rate of the zero-order absorption; RSE, relative SE; T_{lag} (h), the absorption lag time; V_1/f (L/m^2), the apparent volume of sorafenib; V_2/fn (L/m^2), the apparent volumeof sorafenib N-oxide; V_3/fg (L/m^2), the apparent volume of sorafenib glucuronide.

sorafenib N-oxide apparent clearance (Table 2; Supplementary Table S3). The only laboratory result that remained significant relative to the above multivariate model was the bilirubin level. This accounted for an additional 8% and 26% of the IIV in sorafenib N-oxide and sorafenib glucuronide apparent clearance, respectively, relative to the previous model.

A summary of the base and final covariate model results and goodness-of-fit plots for sorafenib, sorafenib N-oxide, and sorafenib glucuronide are shown in Table 2 and Supplementary Fig. S2, respectively. The apparent clearance of sorafenib N-oxide decreased over the period from day 1 to day 7 with daily administration (from a median 27.3 L/hour/m^2 to a median 12.3 L/hour/m^2, $P = 2e{-}5$; Supplementary Fig. S3A). The apparent clearance of sorafenib N-oxide correlated significantly with that of sorafenib ($r = 0.7$, $P = 7e{-}13$), whereas the apparent clearance of sorafenib glucuronide did not correlate with that of the parent compound ($r = 0.06$; $P = 0.6$; Supplementary Fig. S3B and S3C).

A summary of the *post hoc* individual estimated exposure parameters for sorafenib, sorafenib N-oxide, and sorafenib glucuronide on days 1 and 7 is presented in Supplementary Table S5.

Exposure–toxicity association

The determinants of sorafenib-induced HFSR were evaluated using Cox proportional hazards regression analysis. The rate of the first grade 2–3 HFSR was 4.72 times higher (95% CI = 1.81–12.33; $P = 0.0015$) with concurrent administration of clofarabine and cytarabine compared with ANGIO1. However sequential administration of clofarabine and cytarabine versus ANGIO1 was not significantly associated with HFSR (HR = 0.72; 95% CI = 0.22–2.35; $P = 0.591$; Fig. 3A). Next, exposure to sorafenib or its metabolites were considered. Descriptively, patients experiencing grade 2–3 HFSR had higher sorafenib SS trough concentrations when compared with those experiencing grade 0–1 HFSR (median: 4.1 vs. 3.3 mg/L, respectively). A 1,000 ng/mL increase in the sorafenib SS trough concentration was associated with a 1.45-fold increase in the HFSR rate (95% CI = 1.18, 1.78; $P = 0.0004$; Fig. 3B), so the upper quartile concentration associates with an HFSR rate that is 2.16 times that of the lower quartile (95% CI = 1.41–3.32). Patients experiencing grade 2–3 HFSR also had higher sorafenib N-oxide SS trough concentrations when compared with those experiencing grade 0–1 HFSR (median: 0.74 vs. 0.47 mg/L, respectively). In this case, a 100 ng/mL increase in the sorafenib N-oxide SS trough concentration was associated with a 1.04-fold increase in the HFSR rate (95% CI = 1.00, 1.09; $P = 0.0275$; Fig. 3C), so that the upper quartile concentration associates with an HFSR rate that is 1.39 times that of the lower quartile (95% CI = 1.03, 1.86). In addition, each square-meter increase in BSA was associated with an increase in the rate of HFSR by a factor of 2.63 (95% CI = 1.18–5.88; $P = 0.0186$), and after experiencing rash, patients experienced a 2.97-fold increase in the rate of HFSR (95% CI = 1.13–7.79; $P = 0.0268$). Of the 9 patients who had both rash and HFSR, rash was seen before HFSR in 8 patients by a median of 1 day (range, 0–13 days).

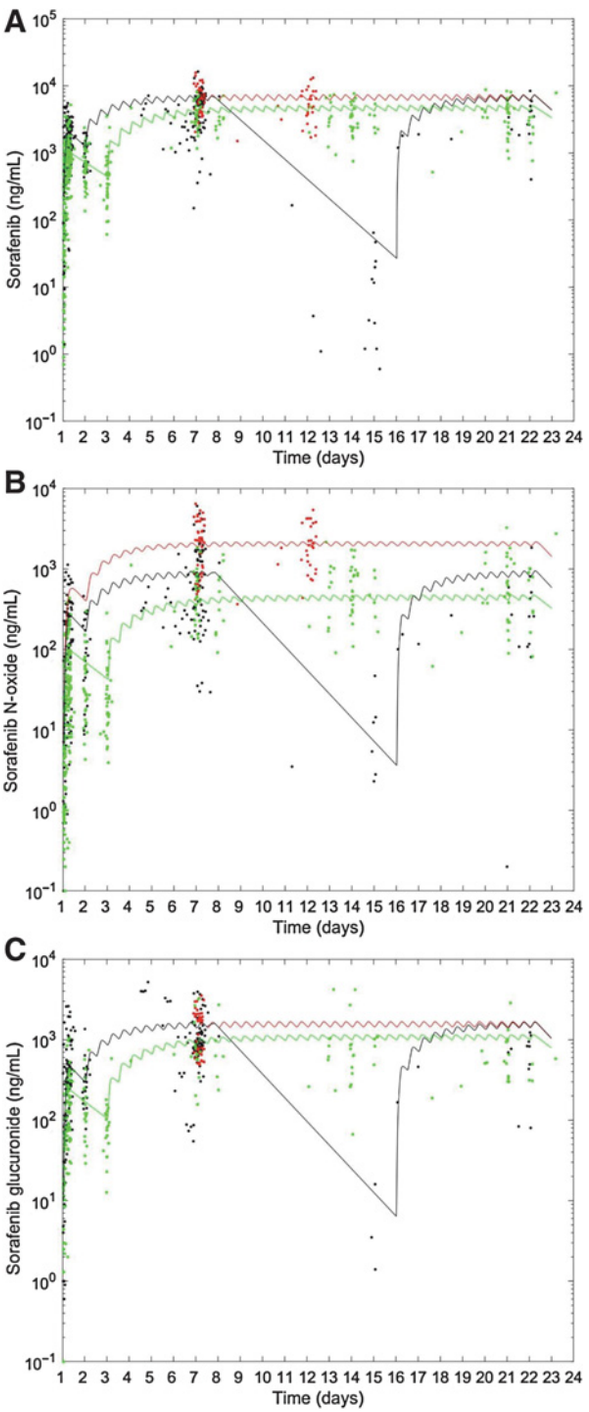

Figure 1.

Population pharmacokinetic model-estimated sorafenib and metabolite concentration-time profiles on different schedules and studies. Concentration-versus-time plots for sorafenib (**A**), sorafenib N-oxide (**B**), and sorafenib glucuronide (**C**). Red curve and symbols: RELHEM with concurrent administration of sorafenib and clofarabine/cytarabine; black curve and symbols, RELHEM with sequential administration of sorafenib and clofarabine/cytarabine; green curve and symbols, ANGIO1.

We next considered models with two predictors. By BIC, the four models with the greatest probability of being the best among those considered are the model with treatment regimen (concurrent or sequential administration with clofarabine and cytarabine vs. ANGIO1) and BSA (47.9% probability); the model with BSA and sorafenib SS trough levels (10.8% probability); the model with treatment regimen and sorafenib SS trough levels (9.1% probability); and the model with prior occurrence of rash and sorafenib SS trough levels (8.8% probability) as predictors of HFSR (Supplementary Table S6). This analysis indicates that HFSR is associated with the concurrent administration with clofarabine and cytarabine, higher sorafenib SS trough levels, larger BSA, and previous occurrence of rash.

The above analysis indicated that rash may be an indicator of an increased risk for subsequent development of HFSR. Therefore, we performed Fine–Gray modeling analyses to evaluate factors that were associated with the development of grade 2–3 rash while treating development of HFSR before rash as a competing event. In this analysis, treatment regimen was significantly associated with the development of rash. Patients treated with concurrent administration of clofarabine and cytarabine developed rash at 21.4 times the rate of ANGIO1 patients (95% CI = 4.71–97.24; $P = 0.0001$). Patients treated with sequential administration with clofarabine and cytarabine regimen developed rash at 4.48 times the rate of ANGIO1 patients (95% CI = 0.88–22.91; $P = 0.071$). A 1,000 ng/mL increase in the sorafenib SS trough concentration was associated with a 1.21-fold increase in the rash rate (95% CI = 0.98–1.48; $P = 0.074$), and a 100 ng/mL increase in the sorafenib N-oxide SS trough concentration was associated with a 1.05-fold increase in the rash rate (95% CI = 1.01–1.10; $P = 0.018$). In a BIC model selection analysis, treatment regimen appeared in all of the top four models (Supplementary Table S6).

We performed pharmacokinetic simulations to evaluate alternative sorafenib administration schedules (once a day and every other day) that would minimize the number of patients whose sorafenib SS trough concentrations reached levels associated with HFSR (Fig. 4). Our simulations indicated that both the once-daily and every-other-day schedules of sorafenib 200 mg/m^2 would minimize exposure to sorafenib SS trough concentrations associated with HFSR in most patients. Specifically, the median sorafenib SS trough concentration decreased from 5,743 to 2,564 or 934 ng/mL when the administration schedule changed from twice-daily to once-daily or every-other-day. This decrease in SS trough concentration corresponds to a 3.35-fold reduction in the HFSR rate when changing from twice-daily to once-daily administration (95% CI: 1.71–6.55) and a 6.71-fold reduction when changing from twice-daily to every-other-day (95% CI: 2.26–16.88). Of relevance to patients with AML and FLT3-ITD mutations, which are a target of sorafenib (5), we found that with once-daily or once-every-other-day administration, the estimated SS trough concentrations at the 10th percentile were well above the sorafenib concentration of 143 ng/mL (308 nmol/L) that inhibited phospho-FLT3 of leukemia samples in a plasma inhibitory assay (30). We used this strategy to treat a patient with FLT3-ITD–positive AML with single-agent sorafenib, and remission was maintained for approximately 1 year (Supplementary Table S7).

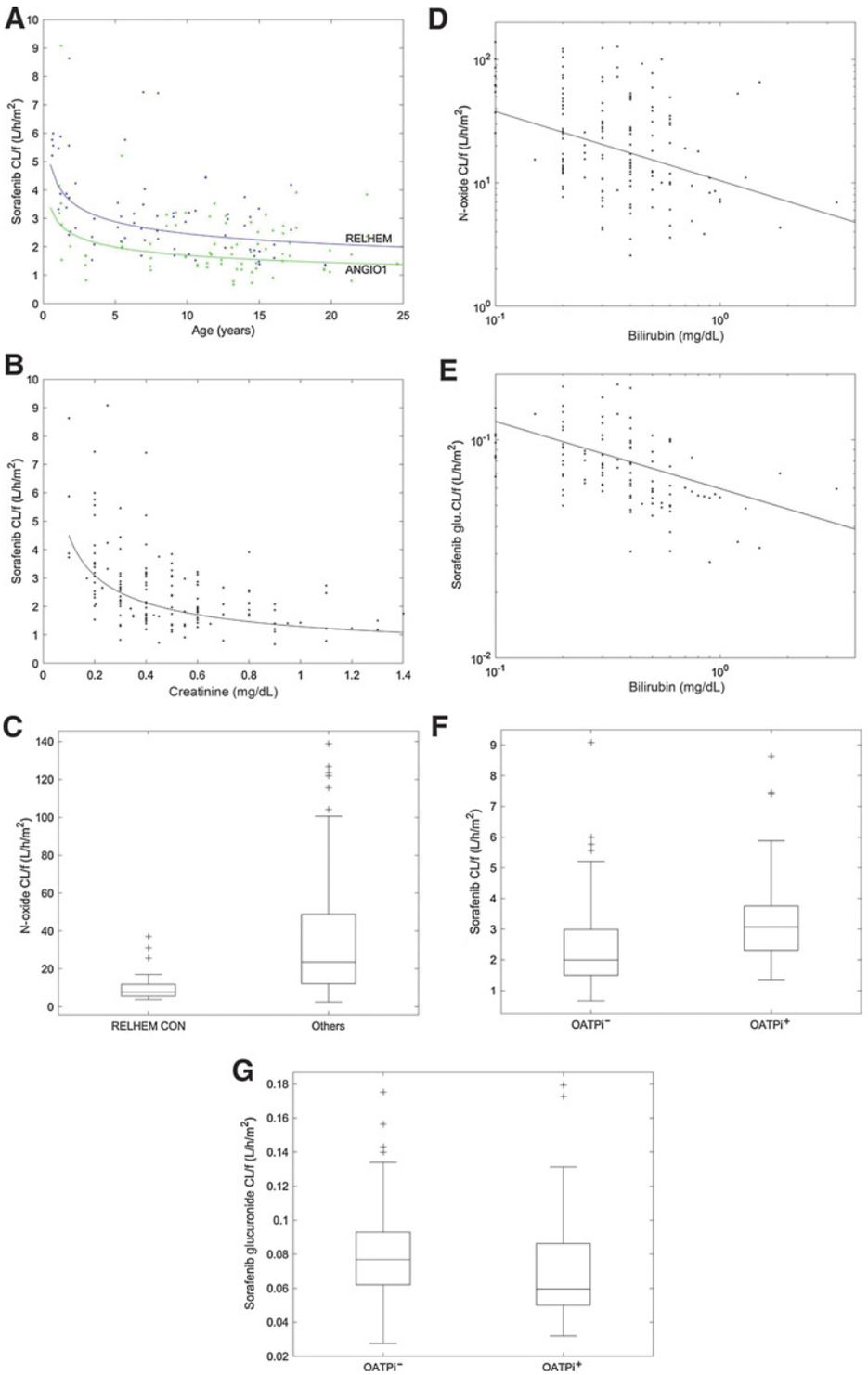

Figure 2.
Association between covariates included in the PPK model and the apparent clearance of sorafenib or its metabolite. **A,** Sorafenib apparent clearance (CL/f) versus age in two studies. Blue curve and symbols, RELHEM ($n = 35$ patients); green curve and symbols, ANGIO1 ($n = 39$ patients). **B,** Sorafenib apparent clearance versus creatinine levels ($n = 74$ patients). **C,** Effects on sorafenib N-oxide apparent clearance of concurrent administration of sorafenib and clofarabine/cytarabine (Clo/AraC) in RELHEM (RELHEM CON; $n = 11$ patients) versus other regimens (sequential administration of sorafenib and clofarabine/cytarabine in RELHEM and ANGIO1; $n = 63$ patients). **D,** Sorafenib N-oxide apparent clearance versus bilirubin levels ($n = 74$ patients). **E,** Sorafenib glucuronide apparent clearance versus bilirubin levels ($n = 74$ patients). **F,** Sorafenib apparent clearance versus OATP1B1 inhibitors (OATPi) ($OATPi^+$, $n = 19$ patients and $OATPi^-$, $n = 55$ patients). **G,** Sorafenib glucuronide apparent clearance versus OATP1B1 inhibitors ($OATPi^+$, $n = 19$ patients and $OATPi^-$, $n = 55$ patients).

Discussion

We have reported the PPK of sorafenib and its metabolites sorafenib N-oxide and sorafenib glucuronide, as well as the skin toxicity, in pediatric patients who were treated with a combination of sorafenib and clofarabine and cytarabine (for leukemia) or a combination of sorafenib and bevacizumab and cyclophosphamide (for solid tumor malignancies). Concurrent administration of sorafenib with clofarabine and cytarabine was associated with skin DLTs in 3 of 6 patients when sorafenib was administered at 200 mg/m^2/day. Sequential administration of clofarabine and

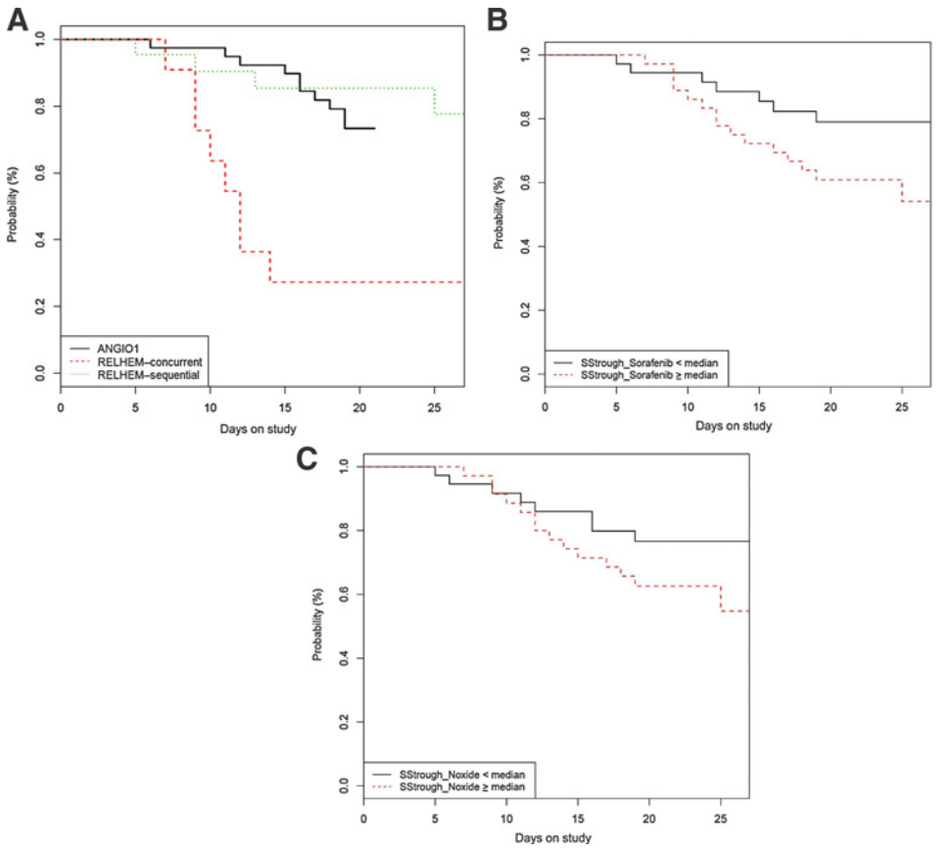

Figure 3.
Grade 2–3 HFSR. **A,** Probability of absence of grade 2–3 HFSR according to the study protocol and the sequence of sorafenib and clofarabine/cytarabine (Clo/AraC) administration. **B** and **C,** The association between exposure to sorafenib (**B**) and sorafenib N-oxide (**C**) and probability of absence of grade 2–3 HFSR. Abbreviations: SStrough_Sorafenib and SStrough_Noxide, steady-state trough concentration of sorafenib and sorafenib N-oxide, respectively.

cytarabine administration and administration of lower sorafenib dose with bevacizumab and cyclophosphamide decreased the onset of HFSR. In the PPK analysis, older age, the study protocol (ANGIO1 vs. RELHEM), and a higher creatinine level were associated with decreased sorafenib apparent clearance and administration of OATP1B1 inhibitors was associated with higher sorafenib apparent clearance. A higher bilirubin level, concurrent administration with clofarabine and cytarabine, and repeated drug administration for 7 days were associated with decreased sorafenib N-oxide apparent clearance. In addition, OATP1B1 inhibitors and increased bilirubin were associated with lower sorafenib glucuronide apparent clearance. In the exposure–toxicity analysis, grade 2–3 HFSR was significantly associated with concurrent administration of clofarabine and cytarabine, higher sorafenib SS trough levels, greater BSA, and previous occurrence of rash and grade 2–3 skin rash was associated with concurrent administration of clofarabine and cytarabine.

This article reports the first PPK model for sorafenib in children. Notably, age was a significant covariate of sorafenib apparent clearance, with younger children exhibiting higher drug clearance than older children. Sorafenib is partly metabolized by CYP3A4 to the active metabolite sorafenib N-oxide and by UGT1A9 to sorafenib glucuronide (6). In young children, CYP450-catalyzed metabolism is increased (31), which could explain the increased sorafenib apparent clearance in younger patients in our PPK model. Greater BSA was associated with higher incidences of HFSR, which may reflect the association of reduced sorafenib clearance (higher exposure) with older age and increasing BSA. The differences in sorafenib apparent clearance between studies could be due to the different cancer types (solid tumor malignancies, which often involve organs, vs. leukemia), the concomitant administration of OATP1B1 inhibitors in RELHEM patients, or differences in concomitant chemotherapy. Because of the small number of each solid tumor subtypes, we were unable to analyze based on the disease subtypes. However, this is the largest available population of pediatric patients with collected pharmacokinetic data. Although urinary excretion plays a minor role in sorafenib and metabolite elimination (accounting for <20% of the total), increased creatinine was associated with decreased apparent clearance of sorafenib. Recently, it has been shown that the clearance of drugs that are substrates for OATP uptake transporters, such as OATP1B1 and OATP1B3, which are located on the sinusoidal membrane of hepatocytes, decreases as kidney function declines (32). We previously demonstrated that sorafenib is a substrate for OATP1B1 and OATP1B3, which may also explain why creatinine is a covariate in the PPK model (33).

We have shown that sorafenib N-oxide also plays an important role in sorafenib-associated skin toxicities, as well as in antileukemia activities as an active metabolite (9, 34). The apparent clearance of sorafenib N-oxide was decreased with higher bilirubin levels and repeated drug administration for 7 days, which could be associated with sorafenib glucuronide, with its high SS concentrations in the liver competing with sorafenib N-oxide for biliary excretion via the efflux transporters ABCB1 and/or ABCC2 (35). It is unclear why there was a difference in sorafenib N-oxide apparent clearance in patients receiving concurrent

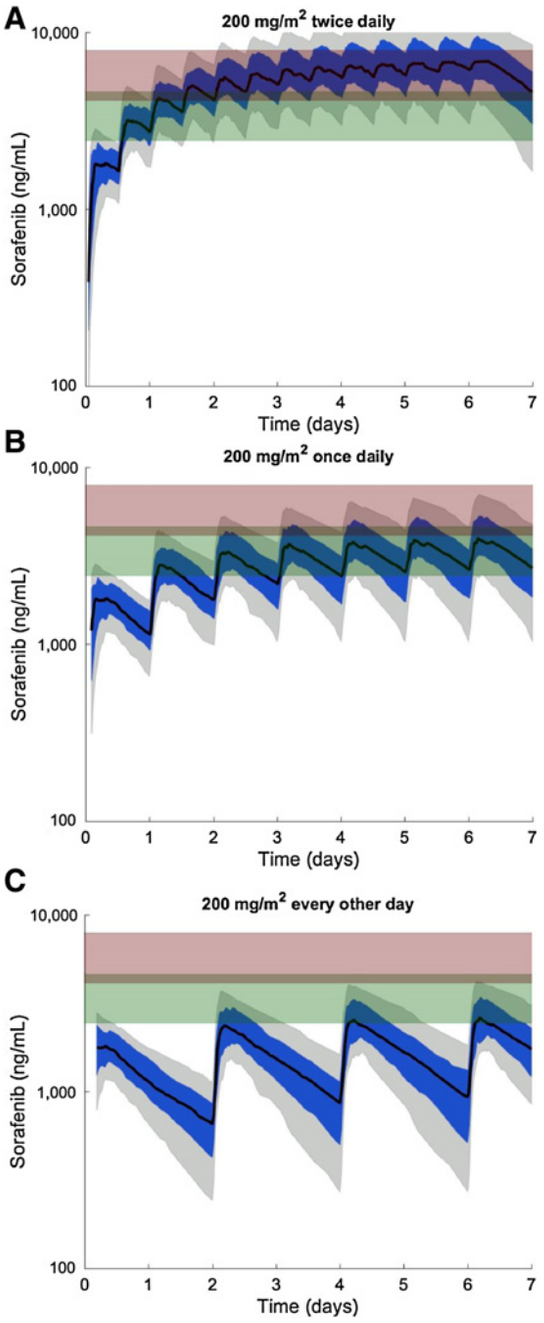

Figure 4.

PPK model simulations of sorafenib plasma exposure on different administration schedules and day 7 trough concentrations associated with HFSR toxicity. Simulations of sorafenib plasma concentrations after the administration of sorafenib at 200 mg/m^2 twice daily (**A**), once daily (**B**), or every other day (**C**). The black curve corresponds to the median concentration. The blue-shaded area corresponds to the 25th to 75th percentiles; the gray-shaded region corresponds to the 10th to 90th percentiles. The green-shaded rectangle corresponds to the 25th to 75th percentiles of the day 7 sorafenib trough concentrations for individuals with grade 0–1 HFSR; the red-shaded rectangle corresponds to the 25th to 75th percentiles of the day 7 sorafenib trough concentrations for individuals with grade 2–3 HFSR.

administration with clofarabine and cytarabine when compared with those in the other group.

In PPK analysis, several variables were associated with sorafenib glucuronide apparent clearance. Bilirubin accounted for a portion (24%) of the variability in the apparent clearance of sorafenib glucuronide. We also showed that concurrent administration of OATP1B1 inhibitors in RELHEM patients was associated with reduced sorafenib glucuronide apparent clearance (higher exposure) and a concomitant increase in sorafenib apparent clearance (lower exposure). This can be explained by inhibition of enterohepatic recirculation of sorafenib glucuronide (by inhibiting liver uptake), which accounts for approximately 50% of the circulating sorafenib parent compound (36). This is the first study to demonstrate a drug–drug interaction between OATP1B1 inhibitors and sorafenib.

The population estimates of sorafenib apparent clearance reported in this study are similar to those reported in several other population pharmacokinetic studies in adults. Specifically, our population estimated apparent clearance of sorafenib in a 10-year-old (the median age of our population) was 2.46 and 1.77 L/h/m^2 in RELHEM and ANGIO1, respectively. The population-estimated apparent clearances of sorafenib reported by Widemann and colleagues (ref. 16; median patient age, 14 years) and Hornecker and colleagues (ref. 37; normalized to a BSA of 2.1) were 3.36 and 1.0 L/hour/m^2, respectively. In addition, the population estimated apparent clearance of sorafenib reported by Jain and colleagues (ref. 36; normalized to a BSA of 2.1 and accounting for the fact that their estimate addressed enterohepatic recirculation) was 1.94 L/hour/m^2. Note that none of these studies measured metabolites.

HFSR is a common adverse event with sorafenib, occurring in approximately 60% of adults treated with this drug, and studies have aimed to identify risk factors for this toxicity, especially for the more severe grades that can decrease the quality of life of patients. Grade 2 or higher HFSR is reported to occur in 36% of patients and typically manifests within the first 2 weeks of treatment (38). The corresponding information on HFSR in pediatric populations is limited, and we observed an increased incidence of grade 2 or higher HFSR (67%) when sorafenib was administered concurrently with clofarabine and cytarabine, with onset occurring during the second week of treatment. The clofarabine and cytarabine regimen is frequently associated with skin toxicity, including palmar–plantar erythrodysesthesia (20, 21), and probably contributed to the increased incidence of HFSR observed during concurrent treatment. In the sequential regimen, the drug holiday between days 8 and 14 led to exposures that were up to three orders of magnitude lower than the corresponding exposures with the concurrent regimen, which can be associated with lower incidences of HFSR. In the ANGIO1 trial, administration of lower doses of sorafenib and bevacizumab and cyclophosphamide, a chemotherapy regimen which has not been associated with skin toxicity, probably contributed to the decreased incidences of HFSR. Although it can be difficult to tease out the role of sorafenib exposure in skin toxicities in the presence of other chemotherapy, sorafenib trough level appeared in three of the top four models by the BIC model selection criteria. One of these top models used treatment regimen and sorafenib trough levels as predictors of HFSR. Therefore, sorafenib exposure, specifically day 7 SS trough concentration, is very likely to be a significant factor associated with HFSR.

In our study, patients with higher SS trough concentrations of sorafenib and sorafenib N-oxide experienced more grade 2 or higher HFSR. Even with the sequential administration of sorafenib in RELHEM or the lower doses of sorafenib in ANGIO1, approximately 20% of patients still experienced HFSR, supporting the importance of trough concentrations. These results are in line with those reported for two previous studies in adults with solid tumors who received single-agent sorafenib therapy, which found an association between a minimal-threshold sorafenib concentration of 5 mg/L or 5.8 mg/L and the incidence of grade 2 or higher HFSR (38, 39). In another study, a nonlinear mixed-effect model was constructed to link sorafenib administration to the risk of HFSR in adults with solid tumors (40). The risk of HFSR increased with the number of doses administered per day (e.g., thrice daily > twice daily > once daily), and this factor was more influential than the total daily dose (range, 200 to 1,600 mg/day). This finding suggests that administering higher daily doses of sorafenib on fewer occasions could minimize the risk of severe HFSR. However, this strategy would need to take into consideration the saturable absorption of sorafenib above single doses of 400 mg (37). Sorafenib is a potent inhibitor of FLT3-ITD–positive AML, and a sorafenib plasma concentration of 143 ng/mL was required to inhibit phospho-FLT3 in a plasma inhibitory assay (30). In this study, the described population model was used to simulate sorafenib exposure with different administration schedules. These simulations suggest that sorafenib can be administered at a dose of 200 mg/m^2 with a reduced frequency of once a day or every other day while maintaining trough concentrations above the threshold needed for the inhibition of FLT3-ITD and avoiding higher concentrations that are associated with HFSR. A similar modeling approach could be used to define alternative sorafenib dosing regimens for children with solid tumors. Further model refinements and the incorporation of physiologically based mechanisms can be used to define exposure–toxicity or exposure–response relationships and to develop alternative dosing strategies for sorafenib (41).

In conclusion, we evaluated the pharmacokinetics and skin toxicity profile of sorafenib administered in combination with clofarabine and cytarabine (either concurrently or sequentially) or bevacizumab and cyclophosphamide. We developed a PPK model for sorafenib and its metabolites in children that identified clinical covariates affecting their apparent clearances. We used the pharmacokinetic model to characterize associations between drug exposure and the dose-limiting toxicity HFSR. In addition, our pharmacokinetic model simulations suggested that an alternative sorafenib treatment regimen has the potential to decrease HFSR while maintaining efficacy, especially in patients with FLT3-ITD–positive AML. This regimen warrants further investigation.

Disclosure of Potential Conflicts of Interest

H. Inaba reports receiving commercial research grants from Bayer/Onyx. No potential conflicts of interest were disclosed by the other authors.

Authors' Contributions

Conception and design: H. Inaba, J. Rubnitz, S.D. Baker
Development of methodology: H. Inaba, J.C. Panetta, S.D. Baker
Acquisition of data (provided animals, acquired and managed patients, provided facilities, etc.): H. Inaba, F. Navid, S.M. Federico. E.D. Eisenmann, A. Vasilyeva, S. Shurtleff, C.-H. Pui, T.A. Gruber, J. Rubnitz
Analysis and interpretation of data (e.g., statistical analysis, biostatistics, computational analysis): H. Inaba, J.C. Panetta, S. Pounds, L. Wang, L. Li, Y.-D. Wang, R.C. Ribeiro, J. Rubnitz, S.D. Baker
Writing, review, and/or revision of the manuscript: H. Inaba, J.C. Panetta, S. Pounds, F. Navid, S.M. Federico, S. Shurtleff, C.-H. Pui, T.A. Gruber, R.C. Ribeiro, J. Rubnitz, S.D. Baker
Administrative, technical, or material support (i.e., reporting or organizing data, constructing databases): H. Inaba, J.C. Panetta, E.D. Eisenmann, A. Vasilyeva, C.-H. Pui
Study supervision: H. Inaba, S.D. Baker

Acknowledgments

We thank the clinical, research, and pharmacokinetic nurses at St. Jude Children's Research Hospital who participated in this study. The research reported in this article was supported by the National Cancer Institute of the NIH [R01CA138744 (to S.D. Baker) and P01CA21765], by ALSAC, and by Bayer/Onyx. We thank Keith A. Laycock, PhD, ELS (St. Jude Children's Research Hospital, Memphis, TN) for editorial assistance.

The costs of publication of this article were defrayed in part by the payment of page charges. This article must therefore be hereby marked *advertisement* in accordance with 18 U.S.C. Section 1734 solely to indicate this fact.

Received February 11, 2019; revised June 7, 2019; accepted August 22, 2019; published first August 27, 2019.

References

1. Zwaan CM, Kolb EA, Reinhardt D, Abrahamsson J, Adachi S, Aplenc R, et al. Collaborative efforts driving progress in pediatric acute myeloid leukemia. J Clin Oncol 2015;33:2949–62.
2. Rubnitz JE. Current management of childhood acute myeloid leukemia. Paediatr Drugs 2017;19:1–10.
3. Smith MA, Altekruse SF, Adamson PC, Reaman GH, Seibel NL. Declining childhood and adolescent cancer mortality. Cancer 2014;120:2497–506.
4. Wilhelm S, Carter C, Lynch M, Lowinger T, Dumas J, Smith RA, et al. Discovery and development of sorafenib: a multikinase inhibitor for treating cancer. Nat Rev Drug Discov 2006;5:835–44.
5. Zhang W, Konopleva M, Shi YX, McQueen T, Harris D, Ling X, et al. Mutant FLT3: a direct target of sorafenib in acute myelogenous leukemia. J Natl Cancer Inst 2008;100:184–98.
6. Zimmerman EI, Roberts JL, Li L, Finkelstein D, Gibson A, Chaudhry AS, et al. Ontogeny and sorafenib metabolism. Clin Cancer Res 2012;18: 5788–95.
7. Borthakur G, Kantarjian H, Ravandi F, Zhang W, Konopleva M, Wright JJ, et al. Phase I study of sorafenib in patients with refractory or relapsed acute leukemias. Haematologica 2011;96:62–8.
8. Ravandi F, Cortes JE, Jones D, Faderl S, Garcia-Manero G, Konopleva MY, et al. Phase I/II study of combination therapy with sorafenib, idarubicin, and cytarabine in younger patients with acute myeloid leukemia. J Clin Oncol 2010;28:1856–62.
9. Inaba H, Rubnitz JE, Coustan-Smith E, Li L, Furmanski BD, Mascara GP, et al. Phase I pharmacokinetic and pharmacodynamic study of the multikinase inhibitor sorafenib in combination with clofarabine and cytarabine in pediatric relapsed/refractory leukemia. J Clin Oncol 2011; 29:3293–300.
10. Röllig C, Serve H, Hüttmann A, Noppeney R, Müller-Tidow C, Krug U, et al. Addition of sorafenib versus placebo to standard therapy in patients aged 60 years or younger with newly diagnosed acute myeloid leukaemia (SORAML): a multicentre, phase 2, randomised controlled trial. Lancet Oncol 2015;16:1691–9.
11. Antar A, Otrock ZK, El-Cheikh J, Kharfan-Dabaja MA, Battipaglia G, Mahfouz R, et al. Inhibition of FLT3 in AML: a focus on sorafenib. Bone Marrow Transplant 2017;52:344–51.
12. Llovet JM, Ricci S, Mazzaferro V, Hilgard P, Gane E, Blanc JF, et al. Sorafenib in advanced hepatocellular carcinoma. N Engl J Med 2008;359:378–90.

13. Cheng AL, Kang YK, Chen Z, Tsao CJ, Qin S, Kim JS, et al. Efficacy and safety of sorafenib in patients in the Asia-Pacific region with advanced hepatocellular carcinoma: a phase III randomised, double-blind, placebo-controlled trial. Lancet Oncol 2009;10:25–34.
14. Escudier B, Eisen T, Stadler WM, Szczylik C, Oudard S, Siebels M, et al. Sorafenib in advanced clear-cell renal-cell carcinoma. N Engl J Med 2007; 356:125–34.
15. Escudier B, Worden F, Kudo M. Sorafenib: key lessons from over 10 years of experience. Expert Rev Anticancer Ther 2019;19:177–89.
16. Widemann BC, Kim A, Fox E, Baruchel S, Adamson PC, Ingle AM, et al. A phase I trial and pharmacokinetic study of sorafenib in children with refractory solid tumors or leukemias: a Children's Oncology Group Phase I Consortium report. Clin Cancer Res 2012;18:6011–22.
17. Navid F, Baker SD, McCarville MB, Stewart CF, Billups CA, Wu J, et al. Phase I and clinical pharmacology study of bevacizumab, sorafenib, and low-dose cyclophosphamide in children and young adults with refractory/recurrent solid tumors. Clin Cancer Res 2013; 19:236–46.
18. Castleberry RP, Crist WM, Holbrook T, Malluh A, Gaddy D. The cytosine arabinoside (Ara-C) syndrome. Med Pediatr Oncol 1981;9:257–64.
19. Cetkovská P, Pizinger K, Cetkovský P. High-dose cytosine arabinoside–induced cutaneous reactions. J Eur Acad Dermatol Venereol 2002;16: 481–5.
20. Faderl S, Verstovsek S, Cortes J, Ravandi F, Beran M, Garcia-Manero G, et al. Clofarabine and cytarabine combination as induction therapy for acute myeloid leukemia (AML) in patients 50 years of age or older. Blood 2006; 108:45–51.
21. Zhang B, Bolognia J, Marks P, Podoltsev N. Enhanced skin toxicity associated with the combination of clofarabine plus cytarabine for the treatment of acute leukemia. Cancer Chemother Pharmacol 2014;74: 303–7.
22. Gomez P, Lacouture ME. Clinical presentation and management of hand-foot skin reaction associated with sorafenib in combination with cytotoxic chemotherapy: experience in breast cancer. Oncologist 2011; 16:1508–19.
23. Anderson RT, Keating KN, Doll HA, Camacho F. The hand-foot skin reaction and quality of life questionnaire: an assessment tool for oncology. Oncologist 2015;20:831–8.
24. Lacouture ME, Wu S, Robert C, Atkins MB, Kong HH, Guitart J, et al. Evolving strategies for the management of hand-foot skin reaction associated with the multitargeted kinase inhibitors sorafenib and sunitinib. Oncologist 2008;13:1001–11.
25. Millisor VE, Roberts JK, Sun Y, Tang L, Daryani VM, Gregornik D, et al. Derivation of new equations to estimate glomerular filtration rate in pediatric oncology patients. Pediatr Nephrol 2017;32:1575–84.
26. Kotsampasakou E, Brenner S, Jäger W, Ecker GF. Identification of novel inhibitors of organic anion transporting polypeptides 1B1 and 1B3 (OATP1B1 and OATP1B3) using a consensus vote of six classification models. Mol Pharm 2015;12:4395–404.
27. De Bruyn T, van Westen GJ, Ijzerman AP, Stieger B, de Witte P, Augustijns PF, et al. Structure-based identification of OATP1B1/3 inhibitors. Mol Pharm 2013;83:1257–67.
28. Karlgren M, Vildhede A, Norinder U, Wisniewski JR, Kimoto E, Lai Y, et al. Classification of inhibitors of hepatic organic anion transporting polypeptides (OATPs): influence of protein expression on drug-drug interactions. J Med Chem 2012;55:4740–63.
29. Burnham KP, Anderson DR. Model selection and multimodel inference: a practical information-theoretic approach. Second edition. New York, NY: Springer; 2002.
30. Pratz KW, Cho E, Levis MJ, Karp JE, Gore SD, McDevitt M, et al. A pharmacodynamic study of sorafenib in patients with relapsed and refractory acute leukemias. Leukemia 2010;24:1437–44.
31. Stewart CF, Hampton EM. Effect of maturation on drug disposition in pediatric patients. Clin Pharm 1987;6:548–64.
32. Tan ML, Yoshida K, Zhao P, Zhang L, Nolin TD, Piquette-Miller M, et al. Effect of chronic kidney disease on nonrenal elimination pathways: a systematic assessment of CYP1A2, CYP2C8, CYP2C9, CYP2C19, and OATP. Clin Pharmacol Ther 2018;103:854–67.
33. Zimmerman EI, Hu S, Roberts JL, Gibson AA, Orwick SJ, Li L, et al. Contribution of OATP1B1 and OATP1B3 to the disposition of sorafenib and sorafenib-glucuronide. Clin Cancer Res 2013;19:1458–66.
34. Zimmerman EI, Gibson AA, Hu S, Vasilyeva A, Orwick SJ, Du G, et al. Multikinase inhibitors induce cutaneous toxicity through OAT6-mediated uptake and MAP3K7-driven cell death. Cancer Res 2016;76:117–26.
35. Vasilyeva A, Durmus S, Li L, Wagenaar E, Hu S, Gibson AA, et al. Hepatocellular shuttling and recirculation of sorafenib-glucuronide is dependent on Abcc2, Abcc3, and Oatp1a/1b. Cancer Res 2015;75:2729–36.
36. Jain L, Woo S, Gardner ER, Dahut WL, Kohn EC, Kummar S, et al. Population pharmacokinetic analysis of sorafenib in patients with solid tumours. Br J Clin Pharmacol 2011;72:294–305.
37. Hornecker M, Blanchet B, Billemont B, Sassi H, Ropert S, Taieb F, et al. Saturable absorption of sorafenib in patients with solid tumors: a population model. Invest New Drugs 2012;30:1991–2000.
38. Karovic S, Shiuan EF, Zhang SQ, Cao H, Maitland ML. Patient-level adverse event patterns in a single-institution study of the multi-kinase inhibitor sorafenib. Clin Transl Sci 2016;9:260–6.
39. Fukudo M, Ito T, Mizuno T, Shinsako K, Hatano E, Uemoto S, et al. Exposure-toxicity relationship of sorafenib in Japanese patients with renal cell carcinoma and hepatocellular carcinoma. Clin Pharmacokinet 2014; 53:185–96.
40. Hénin E, Blanchet B, Boudou-Rouquette P, Thomas-Schoemann A, Freyer G, Vidal M, et al. Fractionation of daily dose increases the predicted risk of severe sorafenib-induced hand-foot syndrome (HFS). Cancer Chemother Pharmacol 2014;73:287–97.
41. Edginton AN, Zimmerman EI, Vasilyeva A, Baker SD, Panetta JC. Sorafenib metabolism, transport, and enterohepatic recycling: physiologically based modeling and simulation in mice. Cancer Chemother Pharmacol 2016;77: 1039–52.